Biomedicine & Pharmacotherapy 132 (2020) 110829

Contents lists available at ScienceDirect

Biomedicine & Pharmacotherapy

journal homepage: www.elsevier.com/locate/biopha

The dual protease inhibitor lopinavir/ritonavir (LPV/r) exerts genotoxic stress on lung cells

Rahaba Marima [a,b,*], Rodney Hull [a], Zodwa Dlamini [a], Clement Penny [b]

[a] SAMRC/UP Precision Prevention and Novel Drug Targets for HIV-Associated Cancers Extramural Unit, Pan African Cancer Research Institute, Faculty of Health Sciences, University of Pretoria, Hatfield, 0028, South Africa
[b] Department of Internal Medicine, School of Medicine, Faculty of Health Sciences, University of the Witwatersrand, Parktown, 2193, South Africa

ARTICLE INFO

Keywords:
Lung cancer
Lopinavir/ritonavir (LPV/r)
DNA Damage Response (DDR) pathway
Genotoxicity
Differential gene expression
Highly Active Antiretroviral Treatment (HAART)
Ingenuity Pathway Analysis (IPA)

ABSTRACT

The Sub-Saharan countries, particularly South Africa has the largest number of people living with HIV, accompanied by the largest antiretroviral treatment (ART) programme in the world. The Highly Active Antiretroviral Treatment (HAART) is the most effective regimen against HIV/AIDS and has improved the lifespan and quality of life of HIV positive patients. HAART has also led to a decrease in the incidence of AIDS defining cancers (ADCs) while there is an increased incidence of the non-AIDS Defining Cancers (NADCs), such as lung cancer in the HAART era. The association between lung tumourigenesis and the use of HAART components such as the dual protease inhibitor (PI) lopinavir/ritonavir (LPV/r) is poorly understood. Using cell and molecular biological approaches, this study aimed at elucidating the effects of LPV/r on the regulation of the cell cycle related genes in normal (MRC-5) and adenocarcinoma (A549) lung cells. Initially, the nuclear integrity of these cells in response to LPV/r was determined using DAPI staining. The effect of LPV/r on cell cycle genes was evaluated through the use of a RT2 PCR gene array of 84 genes related to the cell cycle signaling pathway. The PCR array data was validated by Real-Time Quantification PCR (RT-qPCR). Ingenuity Pathway Analysis (IPA) bio-informatics tool was employed to disclose the molecular mechanism/s observed at cellular and gene expression levels. Loss of nuclear integrity and the upregulation of the p53 DNA damage response (DDR) pathway was revealed by DAPI staining, differential gene expression and IPA core analysis. Furthermore, MAD2L2 and AURKB which also play a role in the DDR pathway were shown to be differentially expressed. The activation of the CASP3 gene in response to LPV/r in A549 cells was also observed. The findings of this study suggest genotoxic properties of LPV/r in healthy normal lung fibroblasts cells and anti-tumour properties in the A549 cells.

1. Introduction

Since the advent of the Highly Active Antiretroviral Treatment (HAART), the quality of life of HIV positive people has improved [1,2]. With over three million patients, the South African national public-sector antiretroviral treatment (ART) programme is the largest in the world [3]. People living with HIV are at an increased risk of developing cancer compared to the general population [4]. This risk may be attributed to viral and bacterial co-infections [5–7]. However, the association between HAART exposure and cancer risk is complex and remains to be elucidated. It is also undetermined yet whether this risk is associated with immunosuppression [4]. This is in light of the HAART associated reduction in the incidence of AIDS defining cancers (ADCs) such as Kaposi sarcoma (KS) and non-Hodgkin lymphoma (NHL) compared to the HAART associated increase in the incidence of non-AIDS defining cancers (NADCs), such as lung cancer [2].

Protease inhibitors remain an integral part of HAART. Lopinavir/Ritonavir (LPV/r) is a dual protease inhibitor (PI) [11]. PIs are essential in HAART regimens and form part of the second line treatment according to WHO [25] guidelines. This dual PI is a second generation PI, which has been shown to have better pharmacological profiles, less severe side effects and demonstrate improved resistance profiles against the multidrug-resistant protease variants compared to first generation PIs [12,13]. However, poor bioavailability and high toxicity are the common disadvantages of PIs. There is therefore an increasing need for the development of next- generation PIs with improved bioavailability

* Corresponding author at: 1SA-MRC/UP Precision Prevention and Novel Drug Targets for HIV-Associated Cancers Extramural Unit, Pan African Cancer Research Institute, Faculty of Health Sciences, University of Pretoria, Hatfield, 0028, South Africa.
E-mail address: rahaba.marima@up.ac.za (R. Marima).

https://doi.org/10.1016/j.biopha.2020.110829
Received 21 May 2020; Received in revised form 6 August 2020; Accepted 28 September 2020
Available online 12 October 2020

and minimal cytotoxicity [27–29]. The cytotoxic effects of PIs has also led to research into the repurposing of ARV drugs as anti-cancer drugs [30]. For example, the cytotoxic effects of nelfinavir, ritonavir, and saquinavir, atazanavir and lopinavir were shown to inhibit protein kinase B (Akt/PKB) and induced caspase-dependent apoptosis [31]. In addition, nelfinavir is undergoing clinical trials as a treatment option against solid tumours [32]. Recently, Mendez-Lopez et al. [33] demonstrated the anti-cancer effects of nelfinavir against multiple myeloma [33]. Furthermore, Kushchayeva et al. [34] reportedthat nelfinavir down-regulates "rearranged during transfection" (RET) signaling and induces apoptosis in medullary thyroid cancer cells [34]. Rizza and Badley [35] described the apoptotic effects of PIs In addition, Tricarico et al. [36] demonstrated the apoptotic properties of LPV/r on neuroblastoma cells (SH-SY5Y) by inducing mitochondrial damage, increase of heme oxygenase RNA expression levels and ROS generation, followed by apoptosis [36]. Kim et al. [37] have also recently reported chemotherapy sensitizing and apoptotic effects of nelfinavir in KBV20C human oral squamous carcinoma cells [37]. With regards to lung cancer, the antitumor effect of nelfinavir on non-small-cell lung cancer (NSCLC) was confirmed *in vivo* using a xenograft model [31,38].

Lung cancer is categorised as non-small-cell lung cancer (NSCLC) and small-cell lung cancer (SCLC), which comprise 85 % and 15 % of all cases, respectively [8]. Deregulation of the cell-cycle and the cell-cycle related components such as p53 and RB have been implicated in lung cancer [9]. Furthermore, the deregulation of the pRB pathway through p16 (CDKI) loss and overexpression of cyclin D1 during the G1 phase is a crucial event during lung carcinogenesis, in both NSCLC and SCLC. The deregulation of the p53 pathway, particularly during the S-phase also plays a key role in lung carcinogenesis [10].

PIs have been reported to have cytotoxic effects [14]. This may compromise genomic integrity, disrupting the cell cycle, causing mutations and cytotoxicity, particularly in normal cells. To protect against genotoxicity, cells initiate the DNA damage response (DDR). This involves activation of signalling cascades, including ATM (ataxia telangiectasia mutated) and p53 signaling pathways [15]. Currently, little is known about how LPV/r induced DNA damage leads to the activation of the DDR signaling pathway. A better understanding of mechanisms whereby this dual PI induces the DDR may lead to the development of countermeasures effective in alleviating genome injury in normal healthy cells. This study aimed at determining the effects of LPV/r on 84 cell cycle related genes in lung cancer. This was accompanied by the evaluation of nuclear integrity in response to LPV/r. *In-silico* bioinformatics analysis was further employed to gain insight to the gene expression and phenotypic patterns observed. Interestingly, the p53 DDR pathway was induced in response to LPV/r. The loss in nuclear integrity in response to LPV/r is attributed here to the upregulation of DDR genes. Such LPV/r targeting of the p53 pathway during the S-phase in lung cells may be key to lung tumourigenesis.

2. Results

2.1. Evaluation of nuclear morphology before and after LPV/r treatment, using DAPI staining

DAPI staining indicated that DNA fragmentation and chromatin condensation occurs in cells treated with LPV/r. Control (vehicle) treated cells did not show signs of DNA fragmentation or chromatin condensation, Fig. 1.

2.2. Profiling of the human cell cycle gene response to LPV/r treatment in human non-small cell lung adenocarcinoma (NSCLC) cells

2.2.1. Human cell-cycle PCR arrays

Following on the aforementioned observations relating to loss of nuclear integrity, a focused gene array panel was employed here to more specifically probe changes in cell cycle related gene expression, in response to LPV/r treatment.

2.3. LPV/r treatment modulate the expression of genes related to the cell cycle in lung cancer cells (A549) and in normal lung cells (MRC-5) groups

Prior to treatment a significant number of genes were shown to be dysregulated, either up or down (Fig. 2A). The upregulated genes (Fig. 2B) included cyclin/CDK complexes, while the down-regulated genes (Fig. 2C) included growth-arrest genes, such as p21 and GADD45A.

LPV/r treatment of MRC-5 cells resulted in the upregulation of the CDKN2B gene Fig. 3A and B and a decreased transcription level of cell-cycle genes assayed (Fig. 3C). In contrast, LPV/r treatment of A549 cells led to a significant dysregulation of the cell-cycle genes assayed. Most of the upregulated genes here (Fig. 4A and B) include the DNA damage

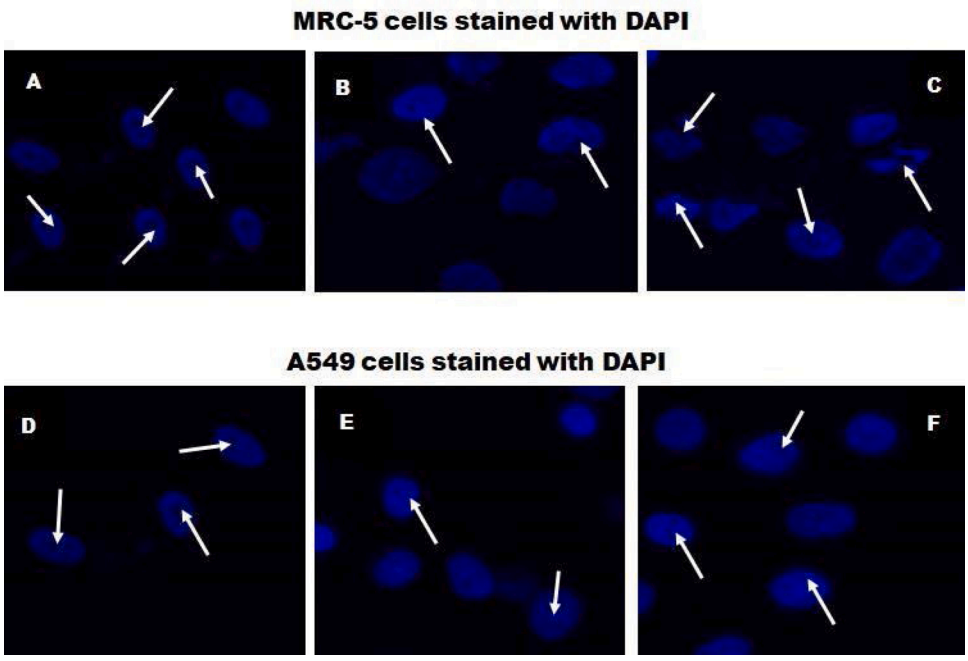

Fig. 1. DAPI staining of MRC-5 and A549 cells in response to LPV/r. Changes in morphology were assessed in LPV/r drug treated relative to control cells. **A** and **D** represent control cells, **B** and **E** show 32μM LPV/r treated cells, while **C** and **F** illustrate 80μM LPV/r treated cells. White arrows point to changes in the nucleus, such as DNA fragmentation and chromatin condensation in LPV/r drug treated (B and C, and E and F), relative to vehicle control cells (A and D) (Original Magnification, 63×).

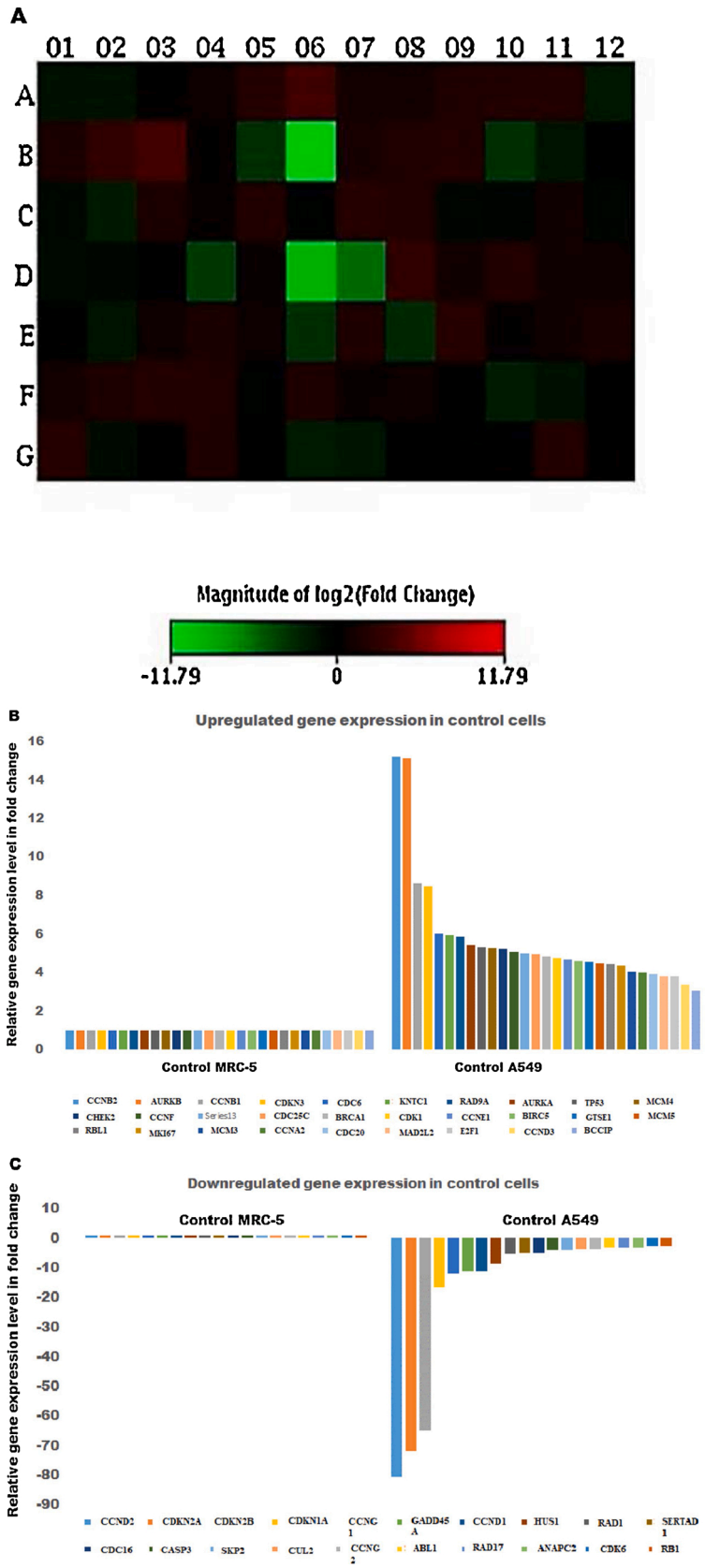

Fig. 2. The cell cycle gene expression profile in control A549 *vs* MRC-5 cells. **A.** The red and green colours in the heat map represent increasing and decreasing gene expression in test group against control group, respectively. **B**. genes that increasedand **C** that decreased, with at least a two-fold differential expression in test against the control group, as represented by the histograms.

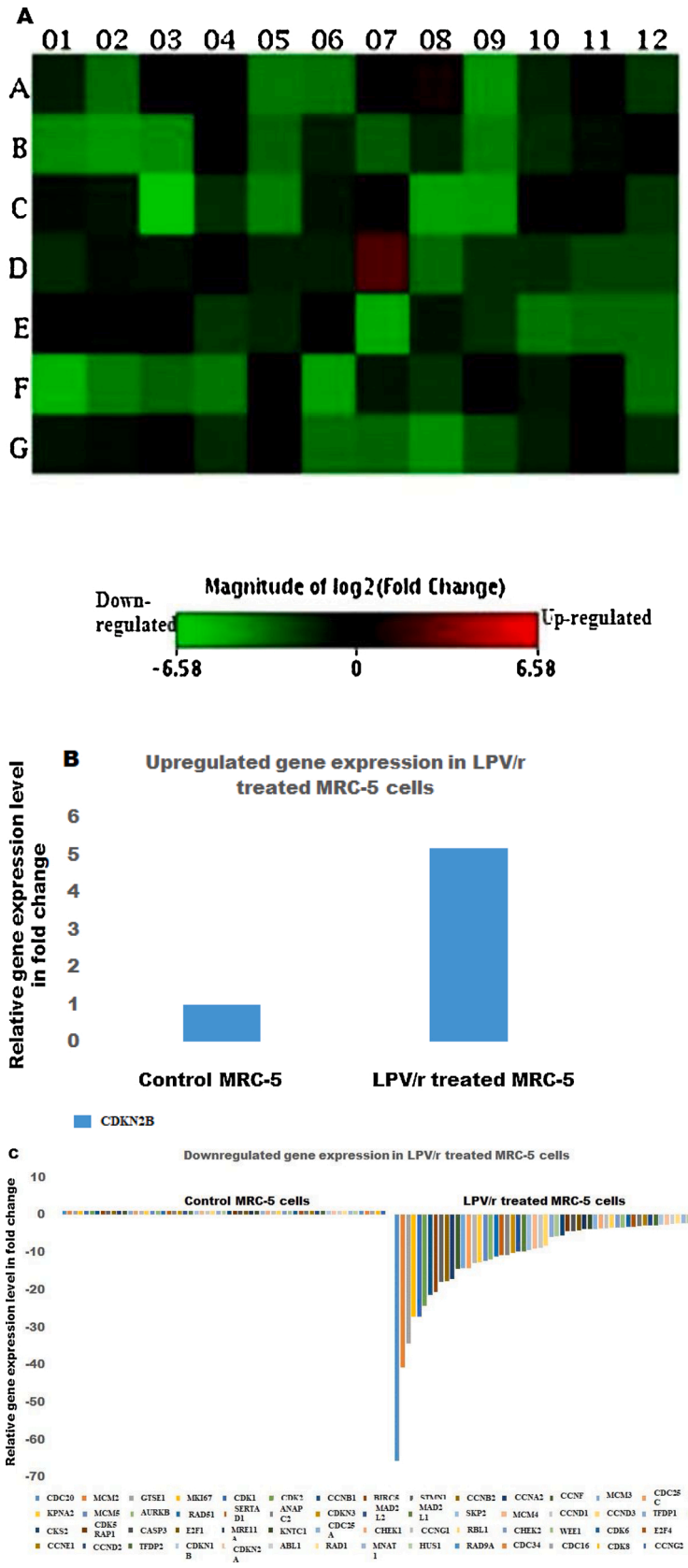

Fig. 3. The cell cycle gene expression profile of LPV/r treated MRC-5 cells. **A**. The red and green colours in the heat map represent increasing or decreasing gene expression in test group against control group. Gene(s) that **B**, increased and **C**, that. decreased, with at least a two-fold differential expression in test (LPV/r treated) against the control group, as demonstrated by the histograms.

response genes ATM, p53 and GADD45A, while the downregulated genes comprising members of the MCM gene family, MAD2L2 and AURKB are shown in Fig. 4C.

2.4. Validation of gene of interest (GOI) using Real-Time quantitative Polymerase Chain Reaction (RT-qPCR)

A number of candidate genes were shown to be differentially expressed, Figs. 2–4. Based on their differential expression across test and control groups, three differentially expressed genes, shown to be either up or down-regulated, were selected, from the gene array studies. The three genes selected were Mitotic Arrest Deficient-Like 2 (MAD2L2) that functions at the cell-cycle checkpoint, Caspase 3 (CASP3) which is apoptosis related and Aurora Kinase B (AURKB), a mitotic gene which attaches the spindle to the centromere.

The transcription level of MAD2L2 was significantly higher in A549 cells as compared to MRC-5. However treatment of MRC-5 and A549 cells with LPV/r led to a significant decrease in the transcription level of MAD2L2. Caspase 3 showed a significant decrease in transcription in A549 cells compared to MRC-5 cells at both 24 and 48 h. LPV/r treatment of MRC-5 treatment led to an increase in transcription of caspase 3 at 24 h, but remained unchanged at 48 h. Finally the transcription of Caspase 3 in A549 cells was insignificantly increased following treatment with LPV/r. The transcription levels of AURKB was higher in A549 cells as compared to MRC-5 cells, Fig. 5. Following treatment of these cells with LPV/r, the transcription of AURKB decreased in both cell lines.

3. Discussion

Even though p53 expression was >2 fold in the tumour *vs* normal cells, p53 downstream effectors such as CDKIs were significantly downregulated, such as p21 at -72 fold. In addition, CASP3 was also shown to be down-regulated. Furthermore, pro-survival genes such as BCL-2 and BIRC-5 (survivin) were also upregulated here. Interestingly, AURK isoforms as well as MAD2L2 (important in mitotic spindle-checkpoint) were revealed as being upregulated, Fig. 6B.

Following lung cell exposure to LPV/r, p53 expression was triggered by decreased levels of AURKB in A549 cells and this in-turn repressed MAD2L2 expression. This was then followed by the activation of downstream targets of p53, including p21, p27 and p16. A significant down-regulation of cyclins A, B, D3, E and F was observed. CDK1 and 2 (except for CDK4) were also down-regulated. E2F1 transcription factor, important for the transcription of S-phase genes was additionally down-regulated. Furthermore, the MCM family of DNA synthesis genes was significantly down-regulated. Survivin (BIRC5) was down-regulated, while CASP3 was up-regulated. The unchanged expression of the BCL-2 gene following LPV/r treatment is obscure here. Unfortunately in this study as part of the array, only the predominant isoform of BCL-2 without a variety of its splice variants was interrogated. Warren et al. [17] reviewed the precise roles of the BCL-2 family isoforms in apoptosis and cancer and identified that there are gaps in the knowledge regarding isoforms of the anti-apoptotic BCL-2 family.

It was then further recommended that studies focusing on understanding the variety of splice variants and isoforms and their biological role in apoptosis is required for targets of the BCL-2 pathway to reach their full potential [16]. Moreover, GADD45A was significantly up-regulated (40 fold). Similarly in MRC-5 cells, insignificant (1.26 fold) p53 activation led to p15 activation, resulting in the inactivation of cyclins/CDKs, deregulation of AURKB and MAD2L2 down-regulation, and a repression in the expression of the MCM gene family, Fig. 6C. LPV/r exhibited characteristics of anti-tumour agents. From this dataset, it is evident that LPV/r induces DNA damage response (DDR) pathways. Furthermore, Aurora kinases and MAD2L2, have previously been shown to be frequently overexpressed in human tumours, causing aberrations in the spindle assembly checkpoint, resulting in chromosomal mis-segregation and centrosome amplification, leading to chromosomal instability and tumorigenesis [17]. Failure to arrest the cell-cycle and repair the DNA damage, may lead to apoptosis. CASP3, an effector caspase important in apoptotic-mediated cell death, was also shown here to be differentially expressed in response to LPV/r drug treatment. De-regulation of CASP3 underlies human diseases including cancer.

MAD2L2 gene also known as REV7 encodes the 211 amino acid MAD2L2 protein and plays an important role in the prevention of the onset of anaphase to permit the correct alignment of all chromosomes at the metaphase plate [18]. MAD2L2 also plays important roles in translesion DNA synthesis, mitotic control, and in repair pathway choice during DNA double-strand breaks. Upon DNA damage, MAD2L2 is recruited to DSB sites, but is not needed to initiate damage signalling. Aurora B forms part of the Chromosome Passenger Complex (CPC) and is partnered with Incenp, Survivin and Borealin. Chromosomal bio-orientation prior to segregation is ensured by AURKB and the CPC. AURKB destabilizes incorrectly attached microtubule (MT)–kinetochore connections via mitotic centromere associated kinesin (MCAK) [19,20]. The phosphorylations (by AURKB) are removed by protein-protein interactions (PPIs), once tension is established and the outer kinetochore is separated from the centromeric Aurora B [21–23]. By generating unattached kinetochores during error correction, Aurora B then affects the spindle assembly checkpoint (SAC) and prevents activation of the anaphase promoting complex/cyclosome (APC/C). Targeted gene expression of S-phase and mitotic checkpoints is observed here. Although the identification of differentially expressed genes is commonly used to explore molecular mechanisms of biological conditions and provides a molecular foothold on biological questions of interest [39]. Protein expression studies could corroborate findings. In particular, the protein expression analysis of DDR components such as MAD2L2 and AURKB whose precise role in DDR remains yet to be elucidated would provide further insights. Additionally, CASP3 cleavage in response to LPV/r treatment would also be beneficial. Therefore, future work may include immunoblot assays for the identified genes of interest, comet assay to quantify genotoxicity, morphological studies of cells in response to LPV/r and posttranscriptional gene regulation, such as miRNA to establish effects of LPV/r on posttranscriptional gene regulation. To our knowledge, this is the first mechanistic study to show the p53 induced DDR in lung cells.

4. Conclusion

It is evident in this study that the DDR genes are upregulated following LPV/r exposure. In addition, the spindle assembly checkpoint (SAC) seems to be targeted by this treatment. This is observed in both normal lung fibroblast and tumour cells, suggesting the cytotoxic role of this dual protease inhibitor not only in cancerous cells, but in healthy cells as well. Although this second generation dual PI has been shown to have improved resistance profiles against HIV, this perhaps warrants the development of next generation PIs that would still be efficient therapies against HIV, but less cytotoxic to normal healthy cells.

5. Experimental procedures

5.1. Drug

Both lopinavir and ritonavir (LPV/r) were purchased from Toronto Research Chemicals (Toronto, Ontario, Canada) and were dissolved in methanol in a 4:1 ratio. A thirty two to eight (32:8 μM) ratio was used as per2019 WHO guidelines [24]. Lopinavir was developed by Abbott to improve upon the properties of ritonavir and was the first dual protease inhibitor available [40–43].

5.2. Cell culture

Cell lines were obtained from the American Type Culture Collection (ATCC) (Manassas, Virginia, United States) and cultured at 37°C in a 5 %

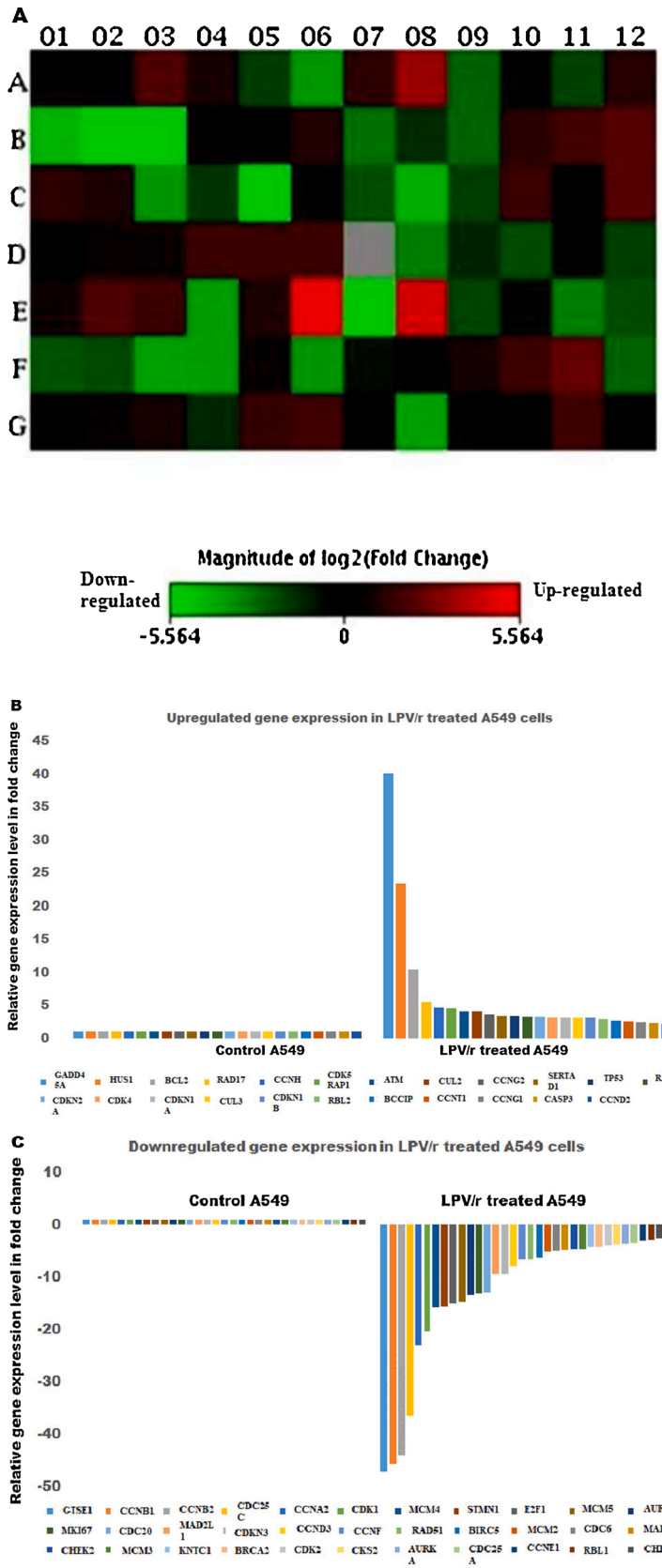

Fig. 4. The cell cycle gene expression profile in LPV/r treated A549 cells. **A**. The red and green colours in the heat map represent increasing or decreasing gene expression in test group against control group, respectively. Genes that increased- **B** and decreased- **C**, with at least a two-fold differential expression in test (LPV/r treated) against the control group, are depicted by the histograms.

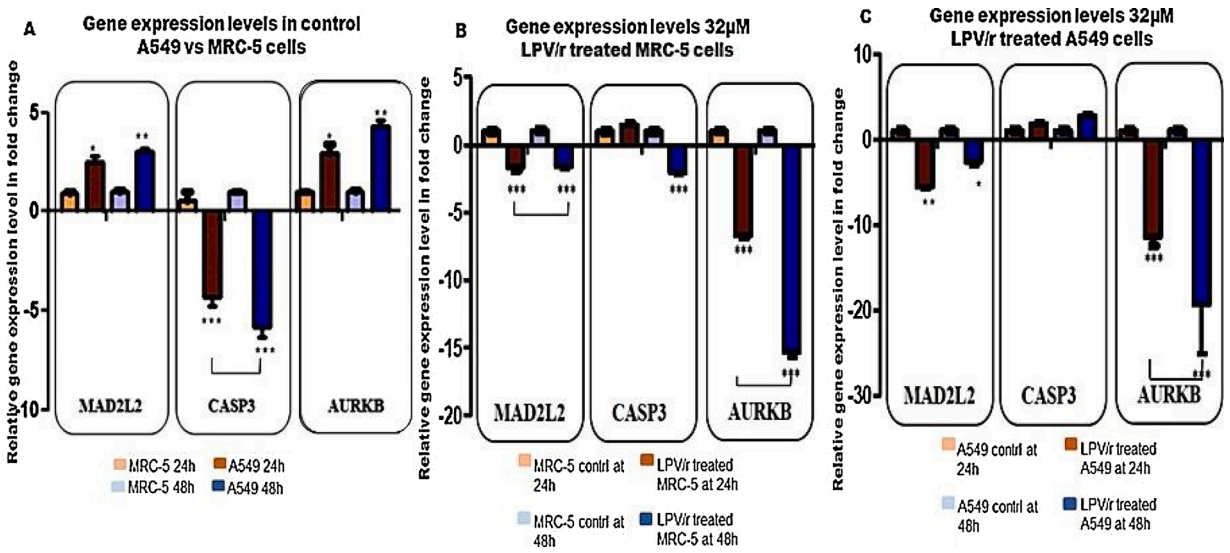

Fig. 5. The validation of GOIs using RT-qPCR at 24 h and 48 h. **A**. Represents target (MAD2L2, CASP3, AURKB) gene expression in fold change in control A549 *vs* MRC-5 cells. **B**. Shows target gene expression in fold change in LPV/r treated MRC-5 cells. **C**. Illustrates target gene expression in fold change in LPV/r A549 cells. All experiments were performed in triplicate at least three times. *p< 0.05, **p < 0.01, ***p < 0.001.

CO_2 incubator. The MRC-5 (ATCC CCL171) and the A549 (ATCC CCL185) cells were grown in Dulbecco's Modified Eagle Medium (DMEM) (Millipore-Sigma, Burlington, Massachusetts, USA) supplemented with 10 % foetal bovine serum (FBS) (Millipore-Sigma, Burlington, Massachusetts, USA) and 1 % penicillin/streptomycin (Thermo Fisher Scientific, Waltham, Massachusetts, USA). For cell cycle PathwayFinder R2 PCR Array (Qiagen, Frederick, Maryland, USA) analysis, the MRC-5 and A549 cells when growing exponentially, were synchronised in the cell cycle by serum starvation and then treated with 32µM LPV/r for 48 h. For the validation study, the control group (vehicle control) was included.

5.3. DNA staining using 4, 6-diamidino-2-phenylindole (DAPI)

DAPI staining was used to assess morphological and nuclear changes such as DNA fragmentation and chromatin condensation in MRC-5 and A549 cells in response to LPV/r. MRC-5 and A549 cells were first fixed by 4 % paraformaldehyde (Millipore-Sigma, Burlington, Massachusetts, USA) in the microfluidic channels at room temperature for 10 min, washed with phosphate buffered saline (PBS) (Millipore-Sigma, Burlington, Massachusetts, USA) three times, permeabilized with 0.3 % Triton X-100 (Millipore-Sigma, Burlington, Massachusetts, USA) for 10 min, washed with PBS (Millipore-Sigma, Burlington, Massachusetts, USA) again three times, and finally stained with 4′,6-diamidino-2-phenylindole (DAPI) for 15 min. The cells were viewed on the Zeiss LSM 780 confocal microscope (Jena, Germany) at 63x magnification.

5.4. RNA isolation, quality control and performance of RT2 qPCR array analysis

RNA isolation was done using an RNeasy Mini kit (Qiagen, Frederick, Maryland, USA) following the manufacturer's instructions. RNA pellets were re-suspended in 30 µl of double distilled H_2O (ddH_2O). RNA yield was quantified using a NanoDrop spectrophotometer (Thermo Fisher, Scientific, Waltham, Massachusetts, USA). For cDNA synthesis, a reverse transcription kit (RT2 First Strand Kit; Qiagen, Frederick, Maryland, USA) was used. The cDNA synthesis reaction was combined with an RT2 SYBR Green qPCR Mastermix (Qiagen, Frederick, Maryland, USA) for loading onto a qPCR array plate. All qPCR array results were obtained using a human cell cycle signaling pathway RT2 Profiler PCR Array of 84 genes (96-well format; PAHS-020Z, Qiagen, Frederick, Maryland, USA). A qPCR components mix, containing RT2 First Strand Synthesis reaction and RT2 SYBR Green Mastermix, was loaded into the array plates with the pre-dispensed primers. The qPCR reactions were performed in a 7500 ABI (Foster City, California, USA) real-time cycler at [10 min at 95 °C, 40 cycles (15 s at 95 °C; 1 min at 60 °C)]. The results of each RT2 Profiler PCR Plate were quality checked by analysing CT values for genomic DNA contamination (GDC), as well as a reverse transcription control (RTC) and positive PCR control (PPC) following the manufacturer's instructions. Each RT2 Profiler PCR Array contains five housekeeping genes (ACTB, B2M, GAPDH, HPRT1, and RPLP0). The geometric mean of the CT values for the five housekeeping genes was calculated and subtracted from the CT value of each gene of interest to obtain ΔCT values. ΔΔCT values were calculated by subtracting the average ΔCT of the control samples from the average ΔCT of the test (LPV/r-treated) samples. Fold changes of gene expression and heatmaps were analyzed and generated by using RT2 PCR array data analysis web portal [25]. Those genes from the 32µM LPV/r treatment groups that had expression fold changes of more than two compared against control groups were considered significant. The candidate genes/ genes of interest (GOI) were chosen to be validated by RT-qPCR.

5.5. Quantitative reverse transcription PCR (RT-qPCR) to validate the PCR array results

Real-Time quantitative Polymerase Chain Reaction (RT-qPCR), was used to assess and confirm the relative gene expression levels of genes of interest (GOI) from the cell-cycle arrays. Total RNA was isolated from MRC-5 and A549 cells using RNeasy Mini kit (Qiagen, Frederick, Maryland, USA)

following the manufacturer's instructions. cDNA was synthesized using the Maxima First Strand cDNA synthesis kit for RT-qPCR with dsDNase (Thermo Fisher Scientific, Waltham, Massachusetts, USA) following the manufacturer's instructions in an ABI 7500 System (Foster City, California, USA). The thermal profile for qPCR was 30 s pre-incubation at 95 °C for one cycle, followed by 40 cycles of 95 °C for 5 s and 60 °C for 34 s. The fold changes amplification for targeted genes was normalized to the housekeeping gene GAPDH by the 2-ΔΔCT method [26]. Fold changes were calculated using Qiagen's web portal and then exported to GraphPad Prism 5, for further statistical analysis, plotting test against control, for all three selected target genes. Results are represented as fold changes in histograms. The following primers

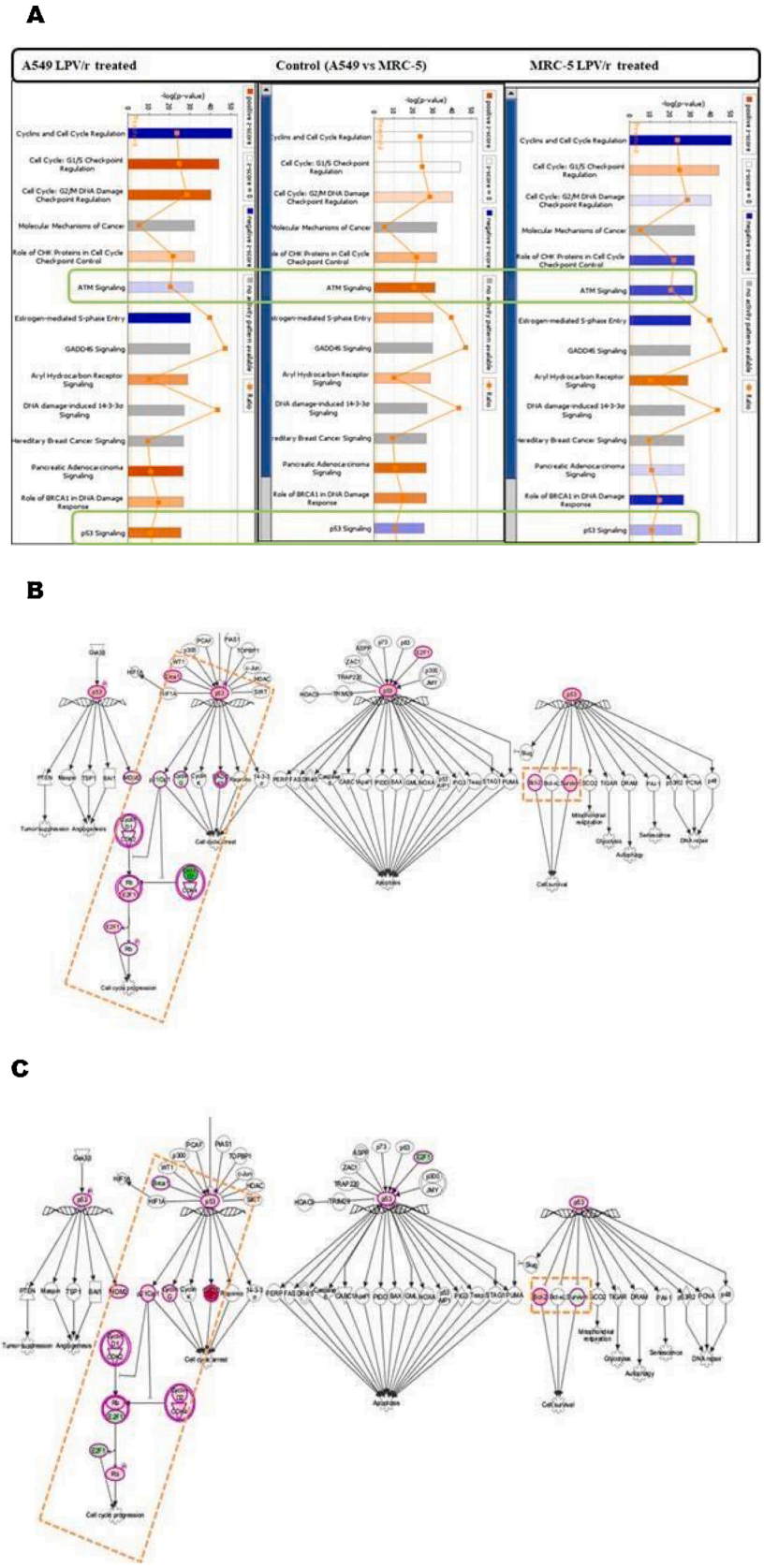

Fig. 6. Ingenuity pathway analysis (IPA) of differential gene expression in response to LPV/r. **A**. Canonical pathway analysis of gene targets in cells treated with 32 μM LPV/r *vs* untreated cells. **B**. IPA p53 signalling pathway in control A549 *vs* MRC-5 cells. The green and red colours represent down and up-regulation. The orange boxes encompass most of the activity in this pathway. **C**. IPA p53-signalling pathway in A549 cells treated with 32 μM LPV/r. The green and the red colours signify down and up- regulation, respectively. The over expression of growth arrest molecules such as p21, Cyclin G and GADD45 in response to the activated p53 is represented here.

were designed by Primer 3 tool (http://primer3.wi.mit.edu/), synthesized by Integrated DNA Technologies (IDT) (Whitehead Scientific, Johannesburg, Gauteng, SA) and were used:

MAD2L2 (NM_006341),

Fwd- CGAGTTCCTGGAGGTGGCTGTGCATC and Rv- CTTGACGCAGTGCAGCGTGTCCTGGATA; **CASP3 (NM_004346)**,

Fwd- GCTCATACCTGTGGCTGTGTA and Rv- ATGAGAATGGGG GAAGAGGCA; **AURKB (NM_004217)**,

Fwd- AGCAGCGAACAGCCACG and Rv- GCCGAAGTCAGCAATCT TCA **GAPDH (NM_002046)**,

Fwd- TGCACCACCAACTGCTTAGC and Rv- GGCATGGACTGTG GTCATGAG.

5.6. Ingenuity pathway analysis (IPA)

Qiagen' s (Frederick, Maryland, USA) Ingenuity Pathways Analysis (IPA) is a web-based bioinformatics application that allows researchers to upload data from gene array analysis for functional analysis, integration, and further understanding. In this study, the IPA canonical pathway analysis and core analysis functions were used. The canonical pathway analysis provides insights into data by determining the most significantly affected pathways. The IPA canonical pathway analysis was used to reveal significantly affected pathways other than the cell cycle in response to LPV/r drug treatment. To achieve this, the z core was primarily used to indicate the degree of expression levels, with positive z score denoting upregulation, negative z core representing downregulation, while zero (0) z core illustrates relatively unchanged gene expression. The core analysis function was used to help build a more complete regulatory picture to better elucidate the biology underlying the studied gene expression profiles in response to LPV/r.

5.7. Statistical analysis

Fold changes of the transcriptional profiling of the 84 genes expression and heatmaps were calculated and generated by using the RT2 PCR array data analysis web portal. Although the RT2 PCR array was performed once per sample, the arrays were validated by a quality check according to the manufacturer's instructions. Genes of the test group (LPV/r treated) compared to control group with differences greater than 2-fold (and $p < 0.05$) were considered significant, as calculated by the RT2 PCR array data analysis web portal. When comparing more than two conditions, data was analyzed by one-way ANOVA, followed by Tukey's *post hoc* test using Graph Pad Prism 5. Values were presented as ±S.E.M for at least three independent experiments. The statistical significance of $p < 0.05$ was considered significant.

Author contributions

Rahaba Marima and Clement Penny conceived and designed the study. Rahaba Marima performed the experiments. Rahaba Marima and Rodney Hull analysed the data. Rahaba Marima and Clement Penny drafted, reviewed and edited the manuscript. Zodwa Dlamini reviewed and edited the manuscript. All authors read and approved the manuscript.

Funding

This work was primarily supported by the South African Medical Research Council (SAMRC).

Declaration of Competing Interest

The authors report no declarations of interest.

Acknowledgments

The authors would like to thank the Cytogenetics Lab (Dr Pascal's Willem Lab), University of the Witwatersrand Medical School for allowing me to use their ABI 7500 RT-qPCR instrument.

References

[1] J. Eriksen, C. Carlander, J. Albert, L. Flamholc, M. Gisslen, L. Naver, V. Svedhem, A. Yilmaz, A. Sonnerborg, Antiretroviral treatment for HIV infection: Swedish recommendations 2019, Infect. Dis. (Lond., Engl.) 52 (2020) 295–329.
[2] M. Corti, Lung cancer in HIV-seropositive patients, MJ HIV 1 (1) (2016) 007.
[3] T. Neluheni, T. Macheka, W. Parker, F. Abdullah, M. Pule, L. Motsieloa, South Africa Global AIDS Response Progress Report (GARPR) 2015, 2019.
[4] Á.H. Borges, Combination antiretroviral therapy and cancer risk, Curr. Opin. HIV AIDS 12 (2017) 12.
[5] L. Albini, A. Calabresi, D. Gotti, A. Ferraresi, A. Festa, F. Donato, M. Magoni, F. Castelli, E. Quiros-Roldan, Burden of non-AIDS-defining and non- virus-related cancers among HIV-infected patients in the combined antiretroviral therapy era, AIDS Res. Hum. Retroviruses 29 (2013) 1097–1104.
[6] M.S. Shiels, R.M. Pfeiffer, M.H. Gail, H.I. Hall, J. Li, A.K. Chaturvedi, K. Bhatia, T. S. Uldrick, R. Yarchoan, J.J. Goedert, E.A. Engels, Cancer burden in the HIV-infected population in the United States, J. Natl. Cancer Inst. 103 (2011) 753–762.
[7] M.J. Silverberg, B. Lau, A.C. Justice, E. Engels, M.J. Gill, J.J. Goedert, et al., Risk of anal cancer in HIV-infected and HIV-uninfected individuals in North America, Clin. Infect. Dis. 54 (2012) 1026–1034.
[8] M.M. Klein, M.B. Moore, R.D. Rodriguez, B. Rourke, S.B. Saag, M.S. Sterling, et al., Risk of anal cancer in HIV-infected and HIV-uninfected individuals in North America, Clin. Infect. Dis. 54 (2012) 1026–1034.
[9] L.C. Wu, Z.S. Wen, Y.T. Qiu, X.Q. Chen, H.B. Chen, M.M. Wei, Z. Liu, S. Jiang, G. B. Zhou, Largazole arrests cell cycle at G1 phase and triggers proteasomal degradation of E2F1 in lung cancer cells, ACS Med. Chem. Lett. 4 (2013) 921–926.
[10] B. Eymin, S. Gazzeri, Role of cell cycle regulators in lung carcinogenesis, Cell Adhesion Migrat. 4 (2010) 114–123.
[11] L. Zhang, J. Zhang, C. Hu, J. Cao, X. Zhou, Y. Hu, Q. He, B. Yang, Efficient activation of p53 pathway in A549 cells exposed to L2, a novel compound targeting p53- MDM2 interaction, Anticancer Drugs 20 (2009) 416–424.
[12] P. Iyidogan, K.S. Anderson, Current perspectives on HIV-1 antiretroviral drug resistance, Viruses 6 (2014) 4095–4139.
[13] S. De Meyer, A. Hill, G. Picchio, R. DeMasi, E. De Paepe, M.P. de Bethune, Influence of baseline protease inhibitor resistance on the efficacy of darunavir/ritonavir or lopinavir/ritonavir in the TITAN trial, J. Acquir. Immune Defic. Syndr. 49 (1999) (2008) 563–564.
[14] P. Grant, E.C. Wong, R. Rode, R. Shafer, A. De Luca, J. Nadler, T. Hawkins, C. Cohen, R. Harrington, D. Kempf, A. Zolopa, Virologic response to lopinavir-ritonavir- based antiretroviral regimens in a multicenter international clinical cohort: comparison of genotypic interpretation scores, Antimicrob. Agents Chemother. 52 (2008) 4050–4056.
[15] D. Maksimovic-Ivanic, P. Fagone, J. McCubrey, K. Bendtzen, S. Mijatovic, F. Nicoletti, HIV-protease inhibitors for the treatment of cancer: repositioning HIV protease inhibitors while developing more potent NO-hybridized derivatives? Int. J. Cancer 140 (2017) 1713–1726.
[16] M. Christmann, B. Kaina, Transcriptional regulation of human DNA repair genes following genotoxic stress: trigger mechanisms, inducible responses and genotoxic adaptation, Nucleic Acids Res. 41 (2013) 8403–8420.
[17] C.F.A. Warren, M.W. Wong-Brown, N.A. Bowden, BCL-2 family isoforms in apoptosis and cancer, Cell Death Dis. 10 (2019) 177.
[18] H. Hochegger, N. Hegarat, J.B. Pereira-Leal, Aurora at the pole and equator: overlapping functions of Aurora kinases in the mitotic spindle, Open Biol. 3 (2013), 120185.
[19] J.E. Sale, REV7/MAD2L2: the multitasking maestro emerges as a barrier to recombination, EMBO J. 34 (2015) 1609–1611.
[20] P.D. Andrews, Y. Ovechkina, N. Morrice, M. Wagenbach, K. Duncan, L. Wordeman, J.R. Swedlow, Aurora B regulates MCAK at the mitotic centromere, Dev. Cell 6 (2004) 253–268.
[21] W. Lan, X. Zhang, S.L. Kline-Smith, S.E. Rosasco, G.A. Barrett-Wilt, J. Shabanowitz, D.F. Hunt, C.E. Walczak, P.T. Stukenberg, Aurora B phosphorylates centromeric MCAK and regulates its localization and microtubule depolymerization activity, Curr. Biol. 14 (2004) 273–286.
[22] M.J. Emanuele, W. Lan, M. Jwa, S.A. Miller, C.S. Chan, P.T. Stukenberg, Aurora B kinase and protein phosphatase 1 have opposing roles in modulating kinetochore assembly, J. Cell Biol. 181 (2008) 241–254.
[23] D. Liu, G. Vader, M.J. Vromans, M.A. Lampson, S.M. Lens, Sensing chromosome bi-orientation by spatial separation of aurora B kinase from kinetochore substrates, Science (New York, N.Y.) 323 (2009) 1350–1353.
[24] D. Liu, M. Vleugel, C.B. Backer, T. Hori, T. Fukagawa, I.M. Cheeseman, M. A. Lampson, Regulated targeting of protein phosphatase 1 to the outer kinetochore by KNL1 opposes Aurora B kinase, J. Cell Biol. 188 (2010) 809–820.
[25] World Health Organisation, Update of Recommendations on First- and Second-Line Antiretroviral Regimens, 2019.
[26] GeneGlobe, K.J. Livak, T.D. Schmittgen, Analysis of relative gene expression data using real- time quantitative PCR and the 2(-Delta Delta C(T)) method, Methods (San Diego, Calif.) 25 (2001) 402–408.

[27] Z. Lv, Y. Chu, Y. Wang, HIV protease inhibitors: a review of molecular selectivity and toxicity, HIV/AIDS (Auckland, N.Z.) 7 (2015) 95–104.
[28] D. Maksimovic-Ivanic, P. Fagone, J. McCubrey, K. Bendtzen, S. Mijatovic, F. Nicoletti, HIV- protease inhibitors for the treatment of cancer: repositioning HIV protease inhibitors while developing more potent NO-hybridized derivatives? Int. J. Cancer 140 (8) (2017) 1713–1726.
[29] M.M. Mudgal, N. Birudukota, M.A. Doke, Applications of click chemistry in the development of HIV protease inhibitors, Int. J. Med. Chem. 2018 (2018), 2946730.
[30] W.B. Bernstein, P.A. Dennis, Repositioning HIV protease inhibitors as cancer therapeutics, Curr. Opin. HIV AIDS 3 (6) (2008) 666–675.
[31] J.J. Gills, J. Lopiccolo, J. Tsurutani, R.H. Shoemaker, C.J. Best, M.S. Abu-Asab, J. Borojerdi, N.A. Warfel, E.R. Gardner, M. Danish, M.C. Hollander, S. Kawabata, M. Tsokos, W.D. Figg, P.S. Steeg, P.A. Dennis, Nelfinavir, a lead HIV protease inhibitor, is a broad-spectrum, anticancer agent that induces endoplasmic reticulum stress, autophagy, and apoptosis in vitro and in vivo, Clin. Cancer Res. 13 (17) (2007) 5183–5194.
[32] National Cancer Institute (NCI), A Phase I Trial of Nelfinavir (Viracept) in Adults with Solid Tumors, 2019 (Accessed 15 March 2019), https://clinicaltrials.gov/ct2/show/NCT00436735.
[33] M. Mendez-Lopez, T. Sutter, C. Driessen, L. Besse, HIV protease inhibitors for the treatment of multiple myeloma, Clin. Adv. Hematol. Oncol. 17 (11) (2019) 615–623.
[34] Y. Kushchayeva, K. Jensen, A. Recupero, J. Costello, A. Patel, J. Klubo-Gwiezdzinska, L. Boyle, K. Burman, V. Vasko, The HIV protease inhibitor nelfinavir down-regulates RET signaling and induces apoptosis in medullary thyroid cancer cells, J. Clin. Endocrinol. Metab. 99 (5) (2014) E734–45.
[35] S.A. Rizza, A.D. Badley, HIV protease inhibitors impact on apoptosis, Med. Chem. (Shariqah (United Arab Emirates)) 4 (1) (2008) 75–79.
[36] P.M. Tricarico, R.F. de Oliveira Franca, S. Pacor, V. Ceglia, S. Crovella, F. Celsi, HIV protease inhibitors apoptotic effect in SH-SY5Y neuronal cell line, Cell. Physiol. Biochem. 39 (4) (2016) 1463–1470.
[37] J.Y. Kim, Y.J. Park, B.M. Lee, S. Yoon, Co-treatment with HIV protease inhibitor nelfinavir greatly increases late-phase apoptosis of drug-resistant KBV20C cancer cells independently of P-glycoprotein inhibition, Anticancer Res. 39 (7) (2019) 3757–3765.
[38] J.J. Gills, J. Lopiccolo, P.A. Dennis, Nelfinavir, a new anti-cancer drug with pleiotropic effects and many paths to autophagy, Autophagy 4 (1) (2008) 107–109.
[39] M. Crow, N. Lim, S. Ballouz, P. Pavlidis, J. Gillis, Predictability of human differential gene expression, Proc. Natl. Acad. Sci. U. S. A. 116 (13) (2019) 6491–6500.
[40] L. Abbott, Laboratories, KALETRA® Product Monographs, 2010, pp. 1–91.
[41] A.K. Ghosh, H.L. Osswald, G. Prato, Recent progress in the development of HIV-1 protease inhibitors for the treatment of HIV/AIDS, J. Med. Chem. 59 (11) (2016) 5172–5208.
[42] L. Palmisano, S. Vella, A brief history of antiretroviral therapy of HIV infection: success and challenges, Annali dell'Istituto superiore di sanita 47 (1) (2011) 44–48.
[43] H.L. Sham, D.J. Kempf, A. Molla, K.C. Marsh, G.N. Kumar, C.M. Chen, W. Kati, K. Stewart, R. Lal, A. Hsu, D. Betebenner, M. Korneyeva, S. Vasavanonda, E. McDonald, A. Saldivar, N. Wideburg, X. Chen, P. Niu, C. Park, V. Jayanti, B. Grabowski, G.R. Granneman, E. Sun, A.J. Japour, J.M. Leonard, J.J. Plattner, D. W. Norbeck, ABT-378, a highly potent inhibitor of the human immunodeficiency virus protease, Antimicrob. Agents Chemother. 42 (12) (1998) 3218–3224.